Observation of All the Intermediate Steps of a Chemical Reaction on an Oxide Surface by Scanning Tunneling Microscopy

Jesper Matthiesen, Stefan Wendt,* Jonas Ø. Hansen, Georg K. H. Madsen, Estephania Lira, Patrick Galliker, Ebbe K. Vestergaard, Renald Schaub, Erik Lægsgaard, Bjørk Hammer,* and Flemming Besenbacher*

Interdisciplinary Nanoscience Center (iNANO) and Department of Physics and Astronomy, Aarhus University, DK-8000 Aarhus C, Denmark

ABSTRACT By means of high-resolution scanning tunneling microscopy (STM), we have revealed unprecedented details about the intermediate steps for a surface-catalyzed reaction. Specifically, we studied the oxidation of H adatoms by O_2 molecules on the rutile TiO_2(110) surface. O_2 adsorbs and successively reacts with the H adatoms, resulting in the formation of water species. Using time-lapsed STM imaging, we have unraveled the individual reaction intermediates of HO_2, H_2O_2, and H_3O_2 stoichiometry and the final reaction product—pairs of water molecules, $[H_2O]_2$. Because of their different appearance and mobility, these four species are discernible in the time-lapsed STM images. The interpretation of the STM results is corroborated by density functional theory calculations. The presented experimental and theoretical results are discussed with respect to previous reports where other reaction mechanisms have been put forward.

KEYWORDS: titania (TiO_2) · oxygen · water · HO_2/H_2O_2 intermediates, hydroxyls · scanning tunneling microscopy (STM) · density functional theory (DFT)

One of the "Holy Grails" within the area of surface science is to directly "watch" chemical reactions at the atomic scale, and STM is the technique of choice for reaching this goal. In the past, the STM has been successfully used to manipulate matter on the atomic scale with single bond precision[1−4] to gain insight into self-diffusion,[5,6] the diffusion of small molecules and adatoms,[7−11] as well as into the diffusion of large organic molecules.[12,13] Moreover, the STM has successfully been used to study spontaneous dissociation reactions of small molecules[14−16] and reactions induced by the tunneling electrons from the STM tip.[4,8,9] For example, the dissociation of O_2 on Pt(111) has been studied by precisely positioning of the STM tip above the O_2 molecule and applying a voltage pulse.[4] However, STM studies unraveling complete surface-catalyzed reactions with all the intermediates are very scarce.

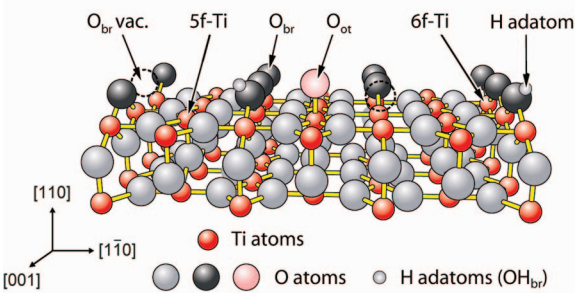

Figure 1. Ball-and-stick model of the TiO_2(110)-(1 × 1) surface with some of its known point defects. Large gray balls represent O atoms, and medium size red balls six-fold coordinated Ti (6f-Ti) and five-fold coordinated surface Ti atoms (5f-Ti), respectively. Small light gray balls represent H adatoms. The bridge-bonded O species (O_{br}), single oxygen vacancies (O_{br} vac.), and the on-top bonded O species (O_{ot}) are also indicated.

Remarkable examples demonstrating how STM can be used to visualize the reactions on metal surfaces have been published by the group of Ertl and Wintterlin.[11,17,18] For instance, Sachs *et al.* studied the catalytic oxidation of hydrogen on Pt(111) and revealed the atomic processes in propagating reaction fronts.[17]

For reactions on oxide surfaces, only few such studies exist.[19−22] With a focus primarily on single crystals, we can restrict ourselves to the very intensely investigated (110) surface of rutile TiO_2 (Figure 1), whose investigations have been triggered through its ease in preparation and numerous applications.[21,23−25] Time-lapsed STM images—in the following referred to as "STM movies"—acquired on this surface at high temperatures provided important information about self-diffusion

*Address correspondence to swendt@phys.au.dk, hammer@phys.au.dk, fbe@inano.dk.

Received for review December 2, 2008 and accepted January 29, 2009.

Published online February 9, 2009.
10.1021/nn8008245 CCC: $40.75

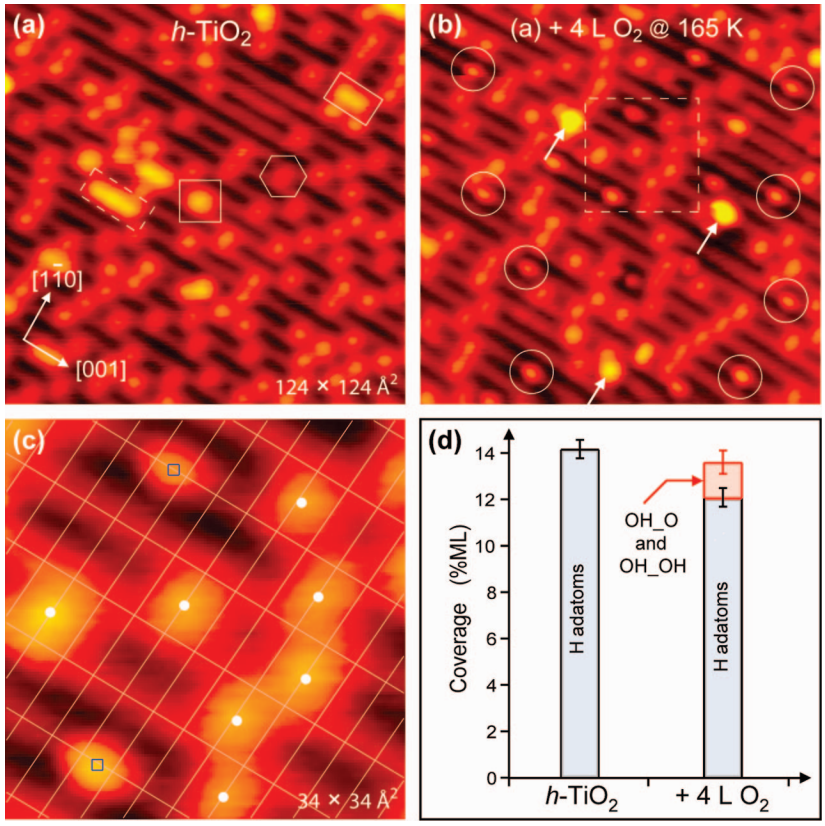

Figure 2. STM images of the *h*-TiO_2(110) surface before (a) and after 4 L O_2 exposure at ~165 K (b). Symbols in (a) indicate single H adatoms (hexagon), paired H adatoms (square), next-nearest H adatoms (rectangle, full line), and a chain of next-nearest H adatoms (rectangle, broken line). The circles in (b) indicate the newly formed species in the Ti troughs, and arrows indicate larger protrusions in the Ti troughs of STM heights as typically observed for water species. The indicated square area in (b) (white broken line) is shown in (c) enlarged. A lattice grid was centered on top of 5f-Ti sites in (c) using single H adatoms (white small dots) for aligning in the [001] direction. Note that the *z* contrast in the STM image depicted in (c) is higher than that in the STM images shown in (a) and (b). The STM images were acquired at 110 K. (d) Bar graph of measured coverages in %ML of the obtained surface species before and after O_2 exposure. To extract the densities of surface species, areas of ~2000 nm^2 were scanned and analyzed.

or the reoxidation of vacuum-annealed TiO_2(110) crystals.[6,26] Onishi and Iwasawa observed the formation of Ti_2O_3 added rows on originally flat (1 × 1) terraces during O_2 exposure of the crystal at 800 K,[6] whereas Bennett *et al.* studied the reoxidation of more reduced TiO_2(110) crystals, whose surfaces showed a (1 × 2) reconstruction.[20,26] In both of these examples, the observed changes on the surface have been explained through the reoxidation of Ti interstitials.

In another example, some of the present authors recorded STM movies at low temperatures (~187 K), showing the dissociation of water molecules in O_{br} vacancies on the TiO_2(110)-(1 × 1) surface.[15] In the same work, it was also shown that water molecules mediate the splitting of OH_{br} pairs that resulted from water dissociation in the O_{br} vacancies into isolated OH_{br} (in the following, we will refer to the OH_{br} groups as H adatoms). Regarding the dissociation of water in O_{br} vacancies, Zhang *et al.* obtained similar results at room temperature (RT) and additionally reported that the resulting two H adatoms in the O_{br} rows behave inequivalently.[27] Moreover, Zhang *et al.* revealed by means of STM that also methanol molecules dissociate in O_{br} vacancies[28] and further that O_{br} vacancies assist the diffusion of alkoxy species along the O_{br} rows.[29]

Much understanding of the chemistry taking place on rutile TiO_2(110) has emerged from these previous studies, highlighting the strength of STM imaging, in particular, if STM movies were successfully recorded. One may, however, object that in all these surface science studies only single reaction steps have been addressed, whereas in "real" catalytic reactions many reaction steps are involved, such as adsorption, diffusion, dissociation, recombination, and desorption. Furthermore, regarding such surface reactions wherein O_{br} vacancies are involved, it can be questioned whether these studies are relevant for "real" catalysis with high pressures of water and other gases. Alone, the fact that it is rather difficult to produce TiO_2(110) surfaces with clean O_{br} vacancies [*r*-TiO_2(110)] even under ultrahigh vacuum (UHV) conditions[30−32] points to a view wherein surface O vacancies are not relevant for real catalysts—simply because they cannot persist under the high pressure conditions. In addition, we have recently found out that the Ti*3d* defect state in the band gap of reduced rutile crystals remains almost unchanged on surfaces without O_{br} vacancies and H adatoms,[33] indicating that the defect state arises not because of these defects as previously believed[21,22,25] but rather from Ti surplus in the near-surface region.[33−35] These results render the study of *r*-TiO_2(110) surfaces with O_{br} vacancies merely of academic interest.

In contrast, the oxidation of H adatoms by O_2 on hydrated TiO_2(110) surfaces [*h*-TiO_2(110)] is both of fundamental as well as practical interest[36] since it involves a common reactant, O_2, and a TiO_2(110) surface in a realistic state without O_{br} vacancies. The practical interest stems primarily from applications in areas such as heterogeneous catalysis[37−39] and photocatalysis[24,25,36] and from the need for an improved understanding of the chemical processes involved in dye-sensitized TiO_2-based solar cells.[23,40] In most of these applications, the presence of O_2 molecules is mandatory.

In this article, we show by means of high-resolution STM studies in conjunction with density functional theory calculations (DFT) that it is possible to follow the intermediate steps of this complex oxidation reaction on the TiO_2(110) surface at the atomic scale. O_2

molecules react with H adatoms on the O_{br} rows, leading to a series of intermediate H transfer reaction steps until the formation of water is complete. STM movies provide a direct view of the reaction, revealing the intermediate steps that take place on the terraces of the oxide surface.

RESULTS AND DISCUSSION

Hydrated and O_2-Exposed, Hydrated TiO_2(110) Surfaces. Figure 2a shows an STM image obtained after hydration of a clean reduced TiO_2(110) surface that was characterized by an O_{br} vacancy density of ~7% ML. In this STM image and in all the following images presented in this article, the imaging mode on the TiO_2(110)-(1 × 1) surface is such that the geometrically protruding O_{br} atoms appear as the dark rows and the Ti troughs as the bright rows.[32,41,42] The bright spots in the dark O_{br} rows arise from single H adatoms[27,30−32] that have been formed due to water dissociation in the O_{br} vacancies[15,22,27,32,43] and subsequent splitting of H adatom pairs mediated by water species.[15] One of the isolated H adatoms in the STM image depicted in Figure 2a is indicated by a hexagon. Additionally, the STM image in Figure 2a shows a few residual pairs of neighboring H adatoms (square), which appear brighter than single H adatoms.[15,30,32] Because H adatoms on next-nearest O_{br} atoms (rectangle, full line) appear also brighter than isolated H adatoms[32] and since the bare O_{br} atoms between two O_{br} atoms capped by H adatoms are not resolved, a chain of H adatoms on next-nearest O_{br} atoms leads to the appearance of elongated bright features in the O_{br} rows (rectangle, broken line).

The STM image depicted in Figure 2b was acquired after 4 L O_2 exposure [1 L (Langmuir) = 1.33 × 10^{-6} mbar · s] at ~165 K to the *h*-TiO_2(110) surface from which we obtained the image shown in Figure 2a. It can be seen that new species with an elongated shape in the [001] direction have formed in the Ti troughs after the O_2 exposure, some of which are indicated by white circles in Figure 2b. In addition, a few very bright features (arrows) have appeared in the Ti troughs that possess STM heights as typically observed for water species.[15,44]

In Figure 2c, we zoom in on the indicated area in Figure 2b for a more detailed analysis. By means of a superimposed grid that was aligned in the [001] direction using the H adatoms, we checked the position of the most abundant new protrusions in the Ti troughs. Because their centers (small blue squares) lie between two intersection points along the [001] direction, it can be concluded that the new species occupy two 5f-Ti sites. The latter also follows when comparing the line profiles of the newly formed species with those of O adatoms, O_{ot}, known from previous studies[30,32,33,45−47] (Figure 3). Because the *h*-TiO_2(110) sample was exposed to O_2, the new species most likely contain two oxygen atoms; however, alone from Figures 2 and 3, it remains

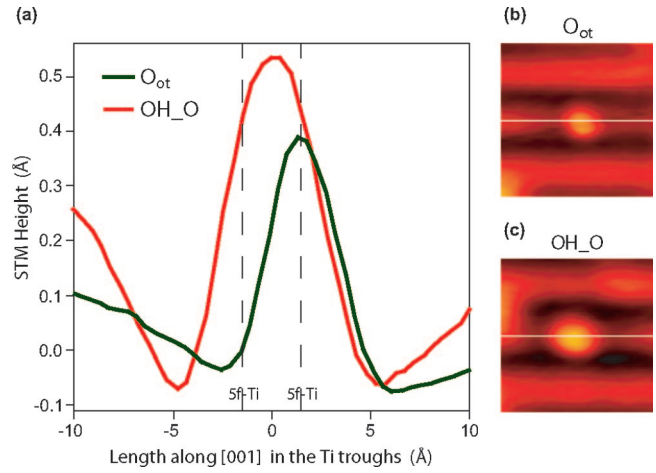

Figure 3. (a) Comparison of the STM height profiles of an O_{ot} adatom (b) and an OH_O species (c) shown in the STM images on the right. Along the [001] direction, OH_O species are centered between two 5f-Ti atoms unlike O_{ot} species that are centered on top of the 5f-Ti atoms. Further evidence for the assignment of the OH_O species is given in the text.

unclear how many H atoms these new species contain. In the experiment described in Figure 2, we detected two different appearances of the new protrusions in the Ti troughs (small blue squares in Figure 2c). Both protrusions are elongated in the [001] direction but have different apparent heights. As will be discussed in the following, this result is related to the number of H atoms contained. In Figure 2c, the bigger protrusion (lower left corner) contains one H more than the species with smaller appearance (upper middle part in the image).

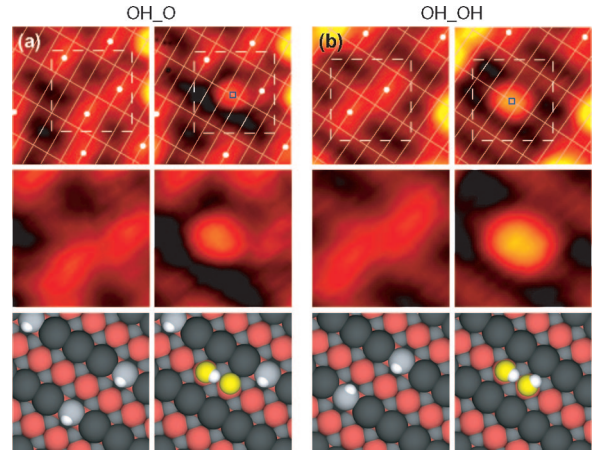

Figure 4. Consecutive STM images (24 × 24 Å^2) acquired from a movie (2.76 s/image) at ~190 K that show the formation of (a) OH_O and (b) OH_OH species. The STM movie was recorded on an *h*-TiO_2(110) with a water coverage of ~6% ML and in an O_2 background of 1 × 10^{-8} Torr. White small dots indicate the positions of H adatoms, and small blue squares are the STM protrusions appearing due to the formation of OH_O and OH_OH species. Areas in the STM images indicated by white dashed squares (13 × 13 Å^2) are shown enlarged in the second row and explained in the third row through ball models (top views). In the ball models, Ti atoms are shown in red and O_{br} atoms in dark gray. The oxygen atoms of the OH_O and OH_OH intermediates are shown in yellow, whereas H atoms are shown as small white balls.

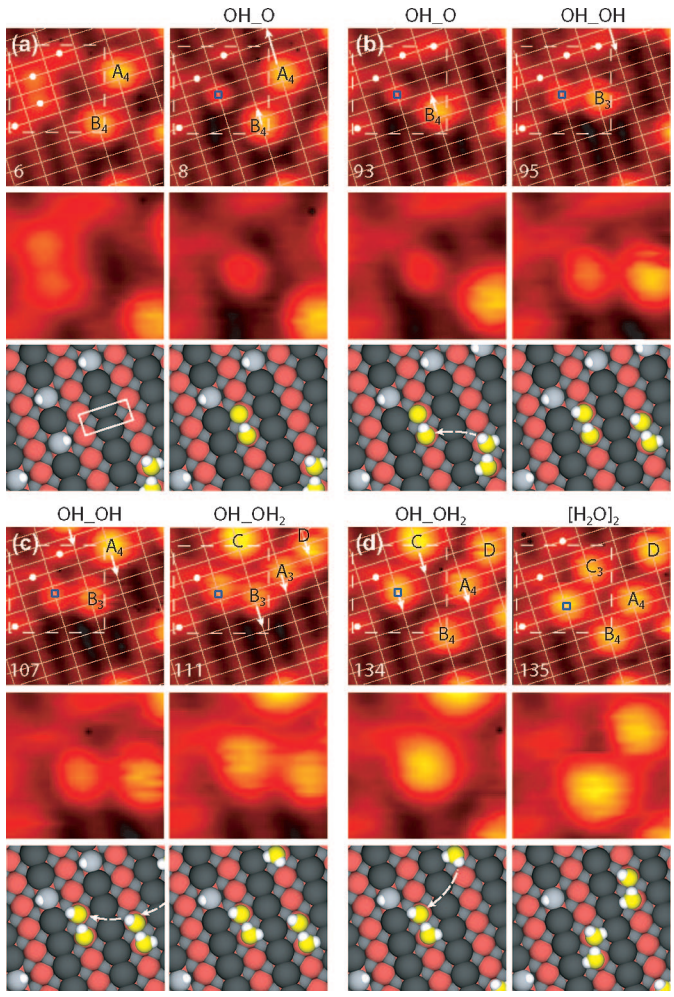

Figure 5. Snapshots extracted from an STM movie "O2_h-TiO2_reaction" recorded on an *h*-TiO_2(110) surface with a water coverage of ~6% ML and in an O_2 background of 1×10^{-8} Torr. The STM images shown in the first row are 30×30 Å^2, but the whole scanned area in the movie was 84×84 Å^2. Images were acquired with a rate of 2.76 s per frame. OH_O formation is shown in (a), and the three following H uptake reactions are identified in (b) OH_OH formation, (c) OH_OH_2 formation, and (d) $[H_2O]_2$ formation, respectively. Numbers at the lower left edges indicate the appearance of the selected STM images within the movie. White small dots indicate H adatoms, and water species in the form of dimers are denoted using the labels A_n, B_n, C_n, and D, respectively, where *n* indicates the estimated number of containing H atoms (*i.e.*, A_n with $n = 4$ denotes a stoichiometric water dimer). In (c) and (d), the index *n* was omitted for some water dimers. The lattice grid is centered on 5f-Ti sites. White arrows along the Ti troughs indicate the diffusion directions of the adsorbates. Indicated areas of 18×16.5 Å^2 size in the STM images in the first row (white dashed rectangles) are shown enlarged in the second row and explained in the third row using ball models (top views). Ti atoms are shown in red and O_{br} atoms in dark gray. The oxygen atoms of the forming water dimer (O_{ad}) are shown in yellow, whereas H atoms are shown as small white balls. The bent arrows indicate from which side in the STM images the H adatoms were provided.

Observations in STM Movies Acquired on Partly Water-Covered *h*-TiO_2(110). To gain more detailed information about the assignment of these new species, we recorded an STM movie on a large terrace on the *h*-TiO_2(110) surface. The STM movie was started before the inlet of O_2 gas through a leak valve was initiated. When stable scanning conditions were achieved, the O_2 background pressure in the chamber was increased and stabilized at ~10^{-8} Torr. In the STM movie, we observed several events as those depicted in Figure 4, where new protrusions appeared in the Ti troughs concomitant with the disappearance of H adatoms on adjacent O_{br} rows. In the first event (Figure 4a), only one H adatom disappeared, whereas in the second event (Figure 4b), two H adatoms disappeared simultaneously as one protrusion appeared in the Ti trough. Events where only one H adatom disappears were observed 10 times during the course of the STM movie, whereas the event shown in Figure 4b where two H adatoms disappear was observed only once. On the basis of these results, we assign the elongated species seen in Figure 2b,c to intermediates with HO_2 and H_2O_2 stoichiometry. This conclusion is consistent with an analysis of the full data set corresponding to the images shown in Figure 2a,b since the total amount of hydrogen before and after the O_2 exposure was found to be identical if we assign the newly found species as species with HO_2 and H_2O_2 stoichiometry (Figure 2d). In the following, we denote the intermediates as OH_O and OH_OH, respectively, because, according to the DFT calculations presented below, the O−O bonds are broken in both of these intermediate species.

We may add that the appearance of the OH_O and OH_OH species in the STM images leads to changes of the STM heights of other adsorbates and of the O_{br} rows. For example, the STM height of the remaining H adatom (right panel in Figure 4a) in the vicinity of the OH_O species is clearly lower than when the OH_O species is not nearby (left panel in Figure 4a). Likewise, the STM height of the O_{br} rows drops in the vicinity of OH_O and OH_OH species, leading to a sombrero-like shape of the adsorbates in the STM images (right panels in Figure 4a,b, respectively). A sombrero-like shape is also evident for the O_{ot} species (Figure 3), suggesting that the decreased STM height in the vicinity of O-containing adsorbates is related to the electronegative character of the adsorbates. These results further underline the now well-established fact that the STM images obtained on the TiO_2(110) surface are strongly influenced by electronic effects.[32,41,42,44]

In the spanned temperature range from ~180 to ~200 K, we observed in the STM movies that the adsorbed OH_O and OH_OH species were immobile. Likewise, the H adatoms that could further react with these intermediates were immobile in this temperature range. This observation suggests that kinetics explains the apparent stability of the OH_O and OH_OH species under the given conditions. However, we know from previous studies that water mediates the net diffusion of H adatoms on *h*-TiO_2(110).[15] In ref 15, the diffusion of H adatoms was reported to occur perpendicularly to the O_{br} rows. Here we observe that under certain conditions water species also mediate the diffusion of H adatoms along the O_{br} rows. In any case, a trace amount of

adsorbed water may facilitate further reactions on the *h*-TiO_2(110) surface.

In another part of the STM movie (the STM movie "O2_h-TiO2_reaction" can be accessed at www.phys.au.dk/spm/movies/O2_h-TiO2_reaction.gif and the Supporting Information), the newly formed OH_O and OH_OH species reacted further in the presence of coadsorbed water species. From an analysis of the STM images acquired before the O_2 exposure, ~6% of the 5f-Ti sites were occupied by H_2O, which was dosed directly after hydration of the TiO_2(110) surface. In Figure 5, water species in the form of dimers are denoted using the labels A_n, B_n, C_n, and D, respectively, where *n* indicates the estimated number of bound H atoms (*i.e.*, A_n with $n = 4$ denotes a stoichiometric water dimer). Starting from OH_O formation, Figure 5a, we identified three additional H uptake reactions: (i) OH_OH formation (Figure 5b), (ii) OH_OH_2 formation (Figure 5c), and finally, (iii) the creation of a water dimer, $[H_2O]_2$ (Figure 5d). Interestingly, we found in the STM movie that upon OH_OH formation the second H stems from a water dimer (denoted as B_4/B_3 in Figure 5b).

It is possible from the high-resolution STM images to identify these reaction intermediates because, upon H uptake (*i.e.*, when OH_O changes to OH_OH and when OH_OH changes to OH_OH_2), the protrusions seen in the STM images always increased (Figure 6). Furthermore, the diffusion rate of the intermediates along the Ti trough differs markedly depending on how many H atoms the intermediate contains. The latter we revealed from several STM movies, one of which was used to extract the data shown in Figure 7. In the experiment corresponding to the data shown in Figure 7, we first exposed an *h*-TiO_2(110) surface to O_2 at RT to decrease the number of H adatoms on the surface[33] before a small amount of water was dosed at ~173 K. In the presented typical example, the mobility of the OH_OH_2 and water dimer species differs by about a factor of 30, which allows us also to differentiate between these two species in the STM movies in spite of their similar STM heights.

We can conclude that the reaction product observed in movie "O2_h-TiO2_reaction" is indeed water in the form of water dimers by comparing the number of reacted O_2 molecules with the number of reacted H adatoms. Figure 8a depicts an STM image from the initial STM movie recorded before the O_2 exposure was initiated. In this STM image, we find a number of water dimers and ~46 H adatoms. The STM image depicted in Figure 8b shows the same surface area as in Figure 8a but 1297 images, that is, 1 h later. While scanning and running the reaction for 1 h, the formation of seven intermediate OH_O species and their further reaction were observed, leading to an increased number of water dimers. Water dimers also diffused into the scanned area from the surrounding area, leading to additional increase in the number of water dimers. Simultaneously, the number of H adatoms in the same surface area has decreased to ~15 (Figure 8b). This result implies that ~4.4 H adatoms have disappeared per O_2 molecule, which is very close to the expected H-to-O_2 ratio of 4:1 according to the proposed reaction pathway.

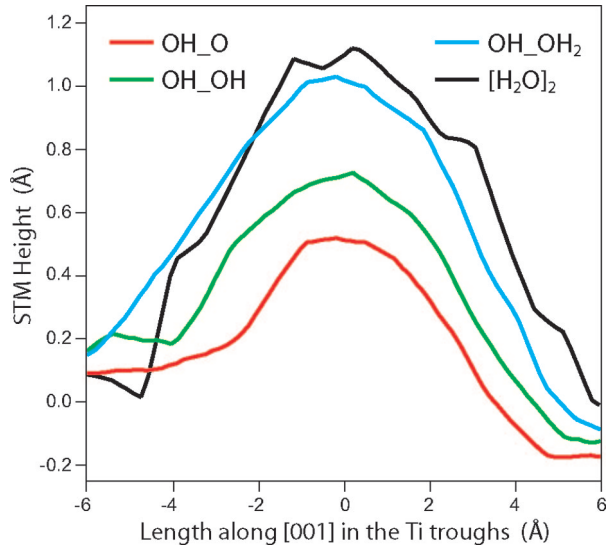

Figure 6. STM height profiles of the OH_O, OH_OH, OH_OH_2, and $[H_2O]_2$ species corresponding to the images shown in Figure 5a, right panel, Figure 5b, right panel, Figure 5d, left panel, and Figure 5d, right panel.

Further STM Experiments Addressing O_2-Exposed TiO_2(110) Surfaces. Because water species in the submonolayer range are known to desorb from vacuum-annealed TiO_2(110) surfaces at ~RT,[36,46,48] newly formed water species, as for instance observed in the STM movie discussed above, should be absent after heating of the sample to temperatures higher than RT. In fact, this situation can be achieved, as is seen from the results depicted in Figure 9. The STM image shown in Figure 9a was acquired subsequently to the experiment de-

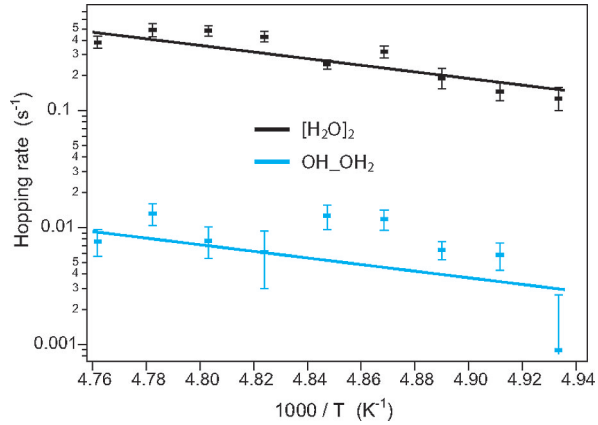

Figure 7. Arrhenius plots for OH_OH_2 and $[H_2O]_2$ species on almost perfect areas on the TiO_2(110) surface. To extract the hopping rates for diffusion along the Ti troughs as a function of temperature only such diffusion events of the OH_OH_2 and $[H_2O]_2$ species were considered when no other species were nearby. The identification of the species rests on typical H transfer and uptake reactions as obtained for the two species considered.

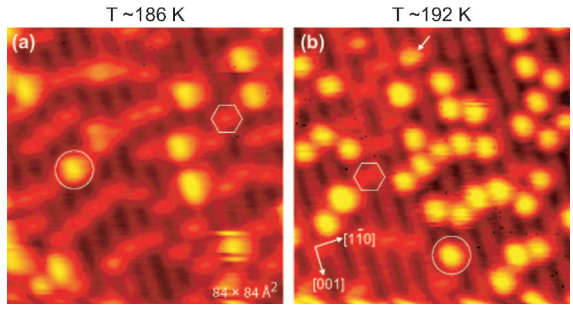

Figure 8. Two STM images acquired within the original STM movie from which we extracted the data presented in Figures 4 and 5 and movie "O2_h-TiO2_reaction". The STM image in (a) was acquired before the O_2 exposure was initiated and at ~186 K. At this time, the number of H adatoms in the scanned area was 46. (b) STM image showing the same surface area as in (a) but 1297 images, that is, 1 h later than the image depicted in (a). This image was acquired with the sample at ~192 K. Symbols indicate H adatoms on O_{br} sites (hexagon) and water dimers in the Ti troughs (circle), respectively. The arrow in (b) indicates a water monomer.

scribed in Figure 2a,b and after heating of the crystal up to ~376 K. Compared to the initial density of H adatoms (~14.2% ML), the density of H adatoms has strongly decreased to ~4.2% ML after heating of the crystal (*cf.* Figure 9b). It appears that the OH_O formation was not complete at 165 K since the density of H adatoms measured directly after the O_2 exposure at 165 K was only slightly decreased. Furthermore, we emphasize that in this experiment, where the O_2 exposure was rather low, no other species in addition to the residual H adatoms were left on the surface after heating. Specifically, we did not find any O_{ot} adatoms or OH_O species on the TiO_2(110) surface (Figure 9a). This result indicates that in the experiment considered all the oxygen atoms that stem from the initially adsorbed and reacted O_2 molecules have left the surface upon heating, most likely in the form of water dimers.

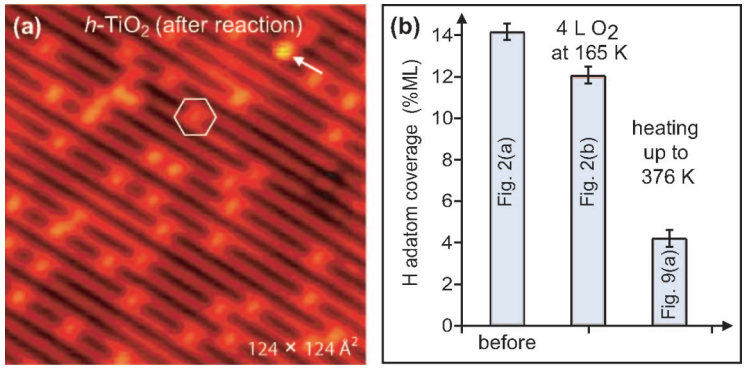

Figure 9. (a) STM image showing the TiO_2(110) after the reaction of O_2 with H adatoms. To initiate the reaction, the *h*-TiO_2(110) surface as depicted in Figure 2a was exposed to 4 L O_2 at ~165 K and then slowly heated up to ~376 K (ramp ~2 K/s). Since the O_2-exposed *h*-TiO_2(110) was inspected by STM (see Figure 2b), it is very likely that trace amounts of water from the background have adsorbed on the surface before the temperature was ramped up to ~376 K. The STM image was acquired at ~110 K. Symbols indicate isolated H adatoms (hexagon) and a water monomer (arrow). (b) Bar graph of measured coverages in %ML of H adatoms before (*cf.* Figure 2a), after O_2 exposure (*cf.* Figure 2b), and after the subsequent heating up to ~376 K. To determine the densities of H adatoms, areas of ~2000 nm² were scanned and analyzed.

Finally, we studied whether O_{ot} adatoms can be reacted off from the TiO_2(110) surfaces when interacting with coadsorbed water and H adatoms. To ensure the availability of H adatoms on the surface, we started with a partly oxidized TiO_2(110) surface that was characterized by the presence of O_{ot} adatoms and O_{br} vacancies (Figure 10a). To prepare such a partly oxidized surface, a clean *r*-TiO_2(110) surface was exposed to 8 L O_2 at RT by backfilling the UHV chamber. In addition to O_{ot} adatoms and O_{br} vacancies, we also find H adatoms on the TiO_2(110) surface. The latter comes about because of the interaction of O_2 molecules with the walls (and other parts) of the UHV chamber, which inevitably leads to an increased partial pressure of water. After water exposure corresponding to a coverage of ~10% ML at ~113 K followed by slowly heating of the crystal up to ~343 K, the result was an *h*-TiO_2(110) surface with a low density of H adatoms (Figure 10b). From this experiment, it is very clear that—through the formation of water—indeed O_{ot} adatoms can be reacted off from the TiO_2(110) surface.

DFT Calculations. To verify the reaction pathway revealed from the STM movie and to clarify the nature of the reaction intermediates, we performed first-principles DFT calculations using the DACAPO package,[49] ultrasoft pseudopotentials, and the revised Perdew−Burke−Ernzerhof (RPBE) exchange−correlation functional.[50] The slabs used in the calculations were composed of six TiO_2 trilayers with $c(4 \times 2)$ surface cells and 2×2 *k*-points. In order to model bulk-reduced samples, a crystallographic shear-plane (CSP)[51,52] parallel to the (110) surface was introduced by removing every second O atom between the fourth and fifth layer of Ti atoms and by shifting the upper four trilayers in the (1)/(2)[0$\bar{1}$1] direction. The distance of the CSP from the (110) surface was chosen such that the energetics of the O_2 adsorption on the surface compares to that of O_2 adsorption on a six trilayer slab containing an isolated Ti interstitial.[33]

Figure 11 presents the calculated energetics (Figure 11a) and adsorption configurations of all reaction intermediates (Figure 11b−h). Starting from the *r*-TiO_2(110) surface ($E = 0$) with two O_{br} vacancies and two H_2O molecules in the gas phase, energy is released upon water dissociation in O_{br} vacancies, leading to two H adatoms per O_{br} vacancy. The potential energy curve continues to go "down hill" upon subsequent O_2 adsorption (Figure 11b), OH_O and OH_OH formation, and further all the way to the final reaction product—a water dimer, $[H_2O]_2$ (Figure 11h). These DFT calculations are consistent with the presented STM results, as well as with previously published spectroscopic evidence of water formation by Henderson *et al.*[36] Both the experimental results as well as the computed energetics presented here are at variance with published theoretical work addressing O_2 adsorption

on the *h*-TiO_2(110) surface.[37,53] This discrepancy we trace back primarily to the fact that the authors of refs 37 and 53 assumed a stoichiometric TiO_2 bulk without extra electrons available.

We also calculated the activation energy barriers, E_a, of interest for the proposed reaction sequence. The transfer of the first H adatom from a position on an O_{br} atom to O_2 (Figure 11b) is hindered by a moderate barrier of $E_a = 0.34$ eV. The resulting π-bonded HO_2 species (Figure 11c) instantly ($E_a = 0.05$ eV) transforms into a σ-bonded HO_2 species (Figure 11d) that dissociates very easily ($E_a = 0.15$ eV). According to the low barriers for the latter two reaction steps, any HO_2 species is very short-lived even at the low temperatures used for the STM measurements. Therefore, our DFT calculations suggest that all reaction intermediates observed in the STM images show species in which the O−O bond has been broken.

In Figure 12, we present simulated STM images using the Tersoff−Hamann formalism[54] of four selected configurations, which we considered in Figure 11. It can be seen that the apparent heights in the simulated STM images mirror very well the ones obtained experimentally. Likewise, the elongated shape in the [001] direction is well reproduced in the STM simulations. It should be noted, however, that in the experiments an average over many different configurations of similar or slightly higher energies is seen, whereas the simulations show the local density of states (DOS) only for one particular configuration. This is one of the reasons why all the simulated STM images show an asymmetry, including those corresponding to the OH_OH species (*cf.* Figure 12b) and to the water dimer (*cf.* Figure 12d), whereas the experimental STM images are symmetric about the [001] direction. Of course, for the configurations shown in Figure 12a,c with a H adatom (H_{ad}) on an O_{br} atom nearby, symmetry about the [001] direction cannot be expected. Within the time scale of STM imaging (several seconds per image), the latter two configurations, OH_O plus a H_{ad} (*cf.* Figure 12a) and H_2O_OH plus a H_{ad} (*cf.* Figure 12c, respectively, cannot be observed. Nevertheless, the presented set of simulated STM images for a series of adsorbates shows that we are now approaching a situation that allows a direct comparison between experimental and theoretical results also for semiconducting TiO_2.

Comparison with Temperature-Programmed Desorption Measurements. The presented STM and DFT results are in good agreement with previously published data using temperature-programmed desorption and electron energy loss measurements.[36] Chemisorbed OH_O is the initial intermediate that is produced *via* H transfer reactions from positions on the O_{br} rows to O_2 molecules, which concomitantly dissociate. With subsequent H transfers, OH_OH species are formed in the Ti troughs, in agreement with previous suggestions[36] [note that in refs 36 and 46 the OH_OH species are denoted as pairs of terminal OH groups (OH_t)]. However, as shown in the present work, the further oxidation can proceed differently than proposed by Henderson *et al.*[36] Mediated by coadsorbed water species that make the diffusion of

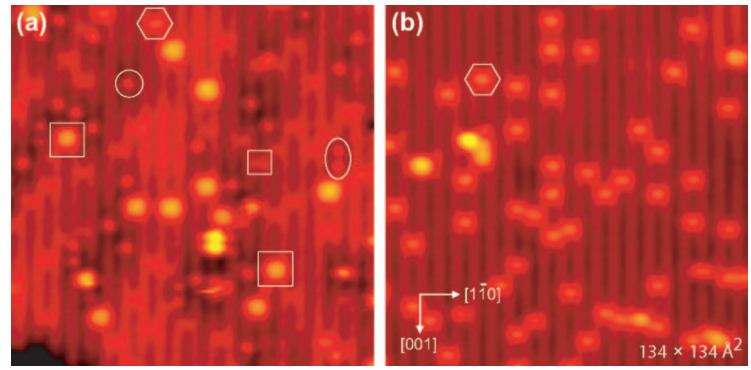

Figure 10. (a) STM image showing a partly oxidized TiO_2(110) surface that was prepared by an O_2 exposure of 8 L at RT to a clean, reduced TiO_2(110) surface. (b) STM image obtained after water exposure corresponding to a coverage of ~10% ML at ~113 K, followed by slowly heating of the crystal up to ~343 K. Symbols indicate O_{br} vacancies (small square), isolated H adatoms (hexagon), paired H adatoms (big square), isolated O_{ot} adatoms (circle), and pairs of next-nearest O_{ot} adatoms (ellipse).

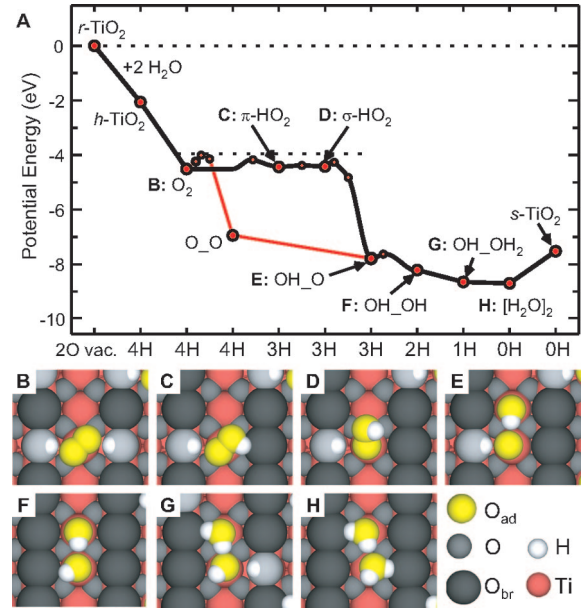

Figure 11. (a) DFT-based potential energy diagram. Big red dots correspond to calculated local potential energy minima, whereas small red dots indicate values deduced using the climbing NEB procedure. The initial configuration is a reduced TiO_2(110) surface [*r*-TiO_2(110)] with two O_{br} vacancies and two H_2O molecules in the gas phase. The first step is dissociation of the H_2O molecules in O_{br} vacancies, thereby forming four H adatoms [*h*-TiO_2(110)] (the number of O_{br} vacancies or H adatoms on the TiO_2(110) surface is denoted on the bottom axis). The second step is the adsorption of an O_2 molecule on *h*-TiO_2(110). The pathway in which O_2 becomes HO_2 before dissociation into OH_O is shown as a thick black line, whereas the thin red line accounts for a pathway in which O_2 dissociates ($E_a = 0.51$ eV) before the reduction. The former pathway is kinetically preferred. Desorption of the $[H_2O]_2$ leads to a clean TiO_2(110) surface, *s*-TiO_2(110), with no point defects in the uppermost surface layer. (b−h) Ball-and-stick models (top views) of selected reaction intermediates. O_{ad} (yellow balls) indicates the O atoms of the adsorbates.

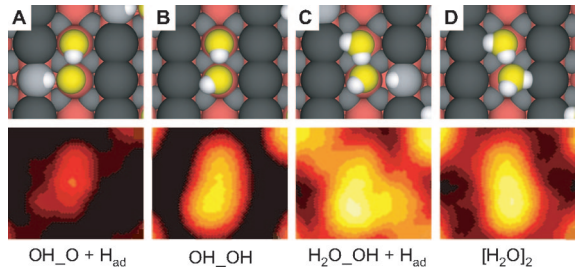

Figure 12. Simulated STM images for selected intermediates together with the corresponding ball-and-stick models: (a) OH_O plus a H adatom (H_{ad}) nearby (*cf.* Figure 11e), (b) OH_OH (*cf.* Figure 11f), (c) H_2O_OH plus a H_{ad} nearby (*cf.* Figure 11g), and (d) $[H_2O]_2$ (*cf.* Figure 11h). In the simulation, the local density of states (DOS) was constructed from electronic states in an energy window between 0.25 and 0.75 eV above the Fermi level (empty states). Isosurfaces of the local DOS are shown for 3×10^{-9} states per Å^3. The color map covers heights in a 2 Å interval; black: ~4 Å, red: ~4.8 Å, orange: ~5.2 Å, yellow: ~5.6 Å, and white: ~6 Å.

H adatoms to O_{br} sites next to the OH_OH species possible, the reaction continues *via* H transfers to the OH_OH species, which finally leads to the formation of water dimers.

Previously, Henderson *et al.* proposed that the OH_OH species decompose into water monomers and O_{ot} adatoms, and that the water monomers desorb at RT, whereas the O_{ot} adatoms remain on the surface.[46] If this were the only possible scenario, heating of an O_2-exposed *h*-TiO_2(110) surface to temperatures higher than RT should always lead to a TiO_2(110) surface with O_{ot} adatoms, irrespectively of the amount of O_2 molecules dosed. As evidenced by the STM image depicted in Figure 9a, no O_{ot} adatoms are left on the surface if small O_2 exposures are used. This means that, as long as sufficient H adatoms are available, the water formation will be completed and thus no O_{ot} adatoms or OH_O species are left on the surface after heating of the crystal to temperatures higher than RT. Despite the fact that the oxidation reaction of H adatoms by O_2 is self-accelerating (the newly formed water species also facilitate the transport of H adatoms toward O_2 and the intermediate species), trace amounts of water must be available on the surface to complete the water formation reaction since without water the H adatoms are immobile at temperatures as high as 200 K.

The presented results are remarkable for at least two reasons. First, the reaction mechanism revealed here for the oxidation reaction of H adatoms by O_2 on TiO_2 mediated by coadsorbed water is interesting, particularly with a view on the promoting role of moisture for catalytic reactions on supported gold clusters[38,55] and the strong indications that the activation of molecular oxygen is the most important reaction step on supported Au nanocatalysts.[37,38] Second, the observed reaction mechanism has presumably universal character for TiO_2 surfaces, meaning that the reaction probably proceeds similarly on other faces of rutile and maybe also on other reducible transition metal oxides. Comparing the available spectroscopic data for TiO_2(110) with those acquired on the (110) face of RuO_2[56,57]—an oxide surface that is isomorphous to the TiO_2(110) surface—some striking similarities are revealed. On both of these surfaces, the transfer of H adatoms from O_{br} sites to oxygen species in the troughs is facile, and in both cases, the formation of water has been observed.

CONCLUSIONS

Unprecedented details about the chemical reaction of O_2 with H adatoms on rutile TiO_2(110) have been revealed by an interplay of time-lapsed, high-resolution STM studies and DFT calculations. O_2 molecules react with H adatoms on the O_{br} rows, leading to a series of intermediate H transfer reaction steps until the formation of water is complete. In order to make the completion of the water formation reaction at temperatures below 200 K possible, the coadsorption of trace amounts of water is required to generate low-barrier pathways for the diffusion of H adatoms. We have shown how the STM with its unique spatial resolution and versatility literally allows us to "watch" a chemical reaction on an oxide surface of high interest.

METHODS

Experimental Details. The experiments were carried out in an ultrahigh vacuum (UHV) chamber with a base pressure in the low 10^{-11} Torr range equipped with a home-built, temperature-variable STM[58,59] and standard facilities for sample preparation and analysis.[60] The sample temperature could be varied from 100 K (by cooling with liquid N_2) to 1200 K by radiative heating and electron bombardment from the back side of the sample; the temperature was measured by a K-type thermocouple spot welded on the sample plate close to the crystal. If the samples were warmed to certain temperatures, we throughout kept the sample for 2 min at the intended temperature to ensure that the crystals reached the temperature measured at the sample plate.

The TiO_2(110)-(1 × 1) samples used for these STM studies were cleaned by several cycles of Ar^+ bombardment at RT and vacuum annealing at 800−950 K. The density of bridging oxygen (O_{br}) vacancies was in the range of 6−8% ML, with 1 ML (monolayer) being the density of the (1 × 1) unit cells, 5.2×10^{14}/cm^2. TiO_2(110) surfaces with H adatoms [*h*-TiO_2(110)] were prepared by water exposure at temperatures ≤170 K to a reduced crystal, followed by slowly warming the crystal up to 373 K. Water exposures were performed *via* background exposure through a leak valve. Several freeze−pump−thaw cycles were performed to purify the deionized water. If not stated otherwise, O_2 was dosed *via* backfilling of the chamber, using a partial O_2 pressure of maximal 5.0×10^{-8} Torr. A cooling trap at the O_2 gas line was used to avoid moisture during O_2 exposure.

The STM images presented in this work were acquired in the constant current mode using a tunneling voltage (V_T) of +1.25 V and a tunneling current (I_T) of ~0.1 nA. A special preamplifier was used, allowing us to work with this low tunnel current and with high feedback gains. Throughout electrochemically etched tungsten tips were used for the STM measurements.

To extract the hopping rates from the STM movies, we first determined so-called displacement distributions from the movies for all the species considered. The displacement distributions, that is, the probabilities for the species to jump 0, 1, 2 *etc.* sites between two successive STM images, were found by comparing the positions of the different species in successive STM images in the STM movies. From these displacement distributions, the hopping rates of the species can be deduced, as described by Ehrlich.[61] For the analysis of the $[H_2O]_2$ diffusion, an average of 540 events was used for each point in the Arrhenius plot, for example, 10 different $[H_2O]_2$ species which were followed on 55 consecutive STM images on average. For the analysis of the OH_OH_2 diffusion, on average, 560 events were used for each of the points in the Arrhenius plot.

Computational Details. The first-principles density functional theory (DFT) calculations were performed using the DACAPO package[50,62] employing plane waves and ultrasoft pseudopotentials. The Ti*3p* states were treated as core states since tests with valence Ti*3p* states showed the energetics to change only little. Exchange−correlation effects were described by the RPBE functional.[50] Slabs of six TiO_2 trilayers with $c(4 \times 2)$ surface cells and 2×2 *k*-points were used. The one-electron states were populated according to a Gaussian broadening scheme with $k_BT = 0.1$ eV. All atoms in the super cell were fully relaxed, and the climbing nudged elastic band (NEB) method[63] was used for determining transition states.

In order to model bulk-reduced samples, a crystallographic shear-plane (CSP)[51,52] parallel to the (110) surface was introduced by removing every second O atom between the fourth and fifth layer of Ti atoms and by shifting the upper four trilayers in the (1)/(2)[0$\bar{1}$1] direction. The distance of the CSP from the (110) surface was chosen such that the energetics of the O_2 adsorption on the surface compares to that of O_2 adsorption on a six trilayer slab with isolated Ti interstitials.[33]

In the calculations addressing adsorbed OH and HO_2 species, we tested the possible influence of spin polarization. However, since the substrate has electrons in gap states right below the conduction band edge, the empty spin states of the adsorbed OH and HO_2 species become filled, leading to vanishing of their net spin moments. Therefore, in subsequent calculations, spin polarization effects could be ignored.

The simulated STM images were constructed as topographs of constant local density of states (3×10^{-9} states per Å^3) according to the Tersoff−Hamann procedure.[54] The local density of states was constructed from electronic states in an energy window between 0.25 and 0.75 eV above the Fermi level (*i.e.*, empty states). The color map covers heights in a 2 Å interval; black: ~4 Å, red: ~4.8 Å, orange: ~5.2 Å, yellow: ~5.6 Å, and white: ~6 Å.

Acknowledgment. We acknowledge financial support from the Danish Ministry of Science, Technology, and Innovation through iNANO, the Danish Research Councils, and the Danish Center for Scientific Computing.

Supporting Information Available: STM movie. This material is available free of charge *via* the Internet at http://pubs.acs.org.

REFERENCES AND NOTES

1. Barth, J. V.; Costantini, G.; Kern, K. Engineering Atomic and Molecular Nanostructures at Surfaces. *Nature* **2005**, *437*, 671–679.
2. Eigler, D. M.; Schweizer, E. K. Positioning Single Atoms with a Scanning Tunneling Microscope. *Nature* **1990**, *344*, 524–526.
3. Gimzewski, J. K.; Joachim, C. Nanoscale Science of Single Molecules Using Local Probes. *Science* **1999**, *283*, 1683–1688.
4. Stipe, B. C.; Rezaei, M. A.; Ho, W.; Gao, S.; Persson, M.; Lundqvist, B. I. Single-Molecule Dissociation by Tunneling Electrons. *Phys. Rev. Lett.* **1997**, *78*, 4410–4413.
5. Horch, S.; Lorensen, H. T.; Helveg, S.; Lægsgaard, E.; Stensgaard, I.; Jacobsen, K. W.; Nørskov, J. K.; Besenbacher, F. Enhancement of Surface Self-Diffusion of Platinum Atoms by Adsorbed Hydrogen. *Nature* **1999**, *398*, 134–136.
6. Onishi, H.; Iwasawa, Y. Dynamic Visualization of a Metal-Oxide-Surface/Gas-Phase Reaction: Time-Resolved Observation by Scanning Tunneling Microscopy at 800 K. *Phys. Rev. Lett.* **1996**, *76*, 791–794.
7. van Gastel, R.; Somfai, E.; van Albada, S. B.; van Saarloos, W.; Frenken, J. W. M. Nothing Moves a Surface: Vacancy Mediated Surface Diffusion. *Phys. Rev. Lett.* **2001**, *86*, 1562–1565.
8. Hla, S.-W.; Rieder, K.-H. STM Control of Chemical Reactions: Single-Molecule Synthesis. *Annu. Rev. Phys. Chem.* **2003**, *54*, 307–330.
9. Ho, W. Single-Molecule Chemistry. *J. Chem. Phys.* **2002**, *117*, 11033–11061.
10. Mitsui, T.; Rose, M. K.; Fomin, E.; Ogletree, D. F.; Salmeron, M. Water Diffusion and Clustering on Pd(111). *Science* **2002**, *297*, 1850–1852.
11. Wintterlin, J. Scanning Tunneling Microscopy Studies of Catalytic Reactions. *Adv. Catal.* **2000**, *45*, 131–206.
12. Kwon, K.-Y.; Wong, K. L.; Pawin, G.; Bartels, L.; Stolbov, S.; Rahman, T. S. Unidirectional Adsorbate Motion on a High-Symmetry Surface: "Walking" Molecules Can Stay the Course. *Phys. Rev. Lett.* **2005**, *95*, 166101.
13. Otero, R.; Hümmelink, F.; Sato, F.; Legoas, S. B.; Thostrup, P.; Lægsgaard, E.; Stensgaard, I.; Galvão, D. S.; Besenbacher, F. Lock-and-Key Effect in the Surface Diffusion of Large Organic Molecules Probed by STM. *Nat. Mater.* **2004**, *3*, 779–782.
14. Mitsui, T.; Rose, M. K.; Fomin, E.; Ogletree, D. F.; Salmeron, M. Dissociative Hydrogen Adsorption on Palladium Requires Aggregates of Three or More Vacancies. *Nature* **2003**, *422*, 705–707.
15. Wendt, S.; Matthiesen, J.; Schaub, R.; Vestergaard, E. K.; Lægsgaard, E.; Besenbacher, F.; Hammer, B. Formation and Splitting of Paired Hydroxyl Groups on Reduced TiO_2(110). *Phys. Rev. Lett.* **2006**, *96*, 066107.
16. Zambelli, T.; Wintterlin, J.; Trost, J.; Ertl, G. Identification of the "Active Sites" of a Surface-Catalyzed Reaction. *Science* **1996**, *273*, 1688–1690.
17. Sachs, C.; Hildebrand, M.; Völkening, S.; Wintterlin, J.; Ertl, G. Spatiotemporal Self-Organization in a Surface Reaction: From the Atomic to the Mesoscopic Scale. *Science* **2001**, *293*, 1635–1638.
18. Wintterlin, J.; Völkening, S.; Janssens, T. V. W.; Zambelli, T.; Ertl, G. Atomic and Macroscopic Reaction Rates of a Surface-Catalyzed Reaction. *Science* **1997**, *278*, 1931–1934.
19. Bonnell, D. A.; Garra, J. Scanning Probe Microscopy of Oxide Surfaces: Atomic Structure and Properties. *Rep. Prog. Phys.* **2008**, *71*, 044501.
20. Bowker, M. The Surface Structure of Titania and the Effect of Reduction. *Curr. Opin. Solid State Mater.* **2006**, *10*, 153–162.
21. Diebold, U. The Surface Science of Titanium Dioxide. *Surf. Sci. Rep.* **2003**, *48*, 53–229.
22. Pang, C. L.; Lindsay, R.; Thornton, G. Chemical Reactions on Rutile TiO_2(110). *Chem. Soc. Rev.* **2008**, *37*, 2328–2353.
23. Grätzel, M. Photoelectrochemical Cells. *Nature* **2001**, *414*, 338–344.
24. Hoffmann, M. R.; Martin, S. T.; Choi, W. Y.; Bahnemann, D. W. Environmental Applications of Semiconductor Photocatalysis. *Chem. Rev.* **1995**, *95*, 69–96.
25. Thompson, T. L.; Yates, J. T. Surface Science Studies of the Photoactivation of TiO_2: New Photochemical Processes. *Chem. Rev.* **2006**, *106*, 4428–4453.
26. Bennett, R. A.; Stone, P.; Price, N. J.; Bowker, M. Two (1×2) Reconstructions of TiO_2(110): Surface Rearrangement and Reactivity Studied Using Elevated Temperature Scanning Tunneling Microscopy. *Phys. Rev. Lett.* **1999**, *82*, 3831–3834.
27. Zhang, Z.; Bondarchuk, O.; Kay, B. D.; White, J. M.; Dohnálek, Z. Imaging Water Dissociation on TiO_2(110): Evidence for Inequivalent Geminate OH Groups. *J. Phys. Chem. B* **2006**, *110*, 21840–21845.

28. Zhang, Z.; Bondarchuk, O.; White, J. M.; Kay, B. D.; Dohnálek, Z. Imaging Adsorbate O−H Bond Cleavage: Methanol on TiO_2(110). *J. Am. Chem. Soc.* **2006**, *128*, 4198–4199.
29. Zhang, Z.; Rousseau, R.; Gong, J.; Li, S.-C.; Kay, B. D.; Ge, Q.; Dohnálek, Z. Vacancy-Assisted Diffusion of Alkoxy Species on Rutile TiO_2(110). *Phys. Rev. Lett.* **2008**, *101*, 156103.
30. Bikondoa, O.; Pang, C. L.; Ithnin, R.; Muryn, C. A.; Onishi, H.; Thornton, G. Direct Visualization of Defect-Mediated Dissociation of Water on TiO_2(110). *Nat. Mater.* **2006**, *5*, 189–192.
31. Suzuki, S.; Fukui, K.; Onishi, H.; Iwasawa, Y. Hydrogen Adatoms on TiO_2(110)-(1 × 1) Characterized by Scanning Tunneling Microscopy and Electron Stimulated Desorption. *Phys. Rev. Lett.* **2000**, *84*, 2156–2159.
32. Wendt, S.; Schaub, R.; Matthiesen, J.; Vestergaard, E. K.; Wahlström, E.; Rasmussen, M. D.; Thostrup, P.; Molina, L. M.; Lægsgaard, E.; Stensgaard, I.; Hammer, B.; Besenbacher, F. Oxygen Vacancies on TiO_2(110) and Their Interaction with H_2O and O_2: A Combined High-Resolution STM and DFT Study. *Surf. Sci.* **2005**, *598*, 226–245.
33. Wendt, S.; Sprunger, P. T.; Lira, E.; Madsen, G. K. H.; Li, Z.; Hansen, J. O.; Matthiesen, J.; Blekinge-Rasmussen, A.; Lægsgaard, E.; Hammer, B.; Besenbacher, F. The Role of Interstitial Sites in the Ti3d Defect State in the Band Gap of Titania. *Science* **2008**, *320*, 1755–1759.
34. Henderson, M. A. A Surface Perspective on Self-Diffusion in Rutile TiO_2. *Surf. Sci.* **1999**, *419*, 174–187.
35. Nolan, M.; Elliott, S. D.; Mulley, J. S.; Bennett, R. A.; Basham, M.; Mulheran, P. Electronic Structure of Point Defects in Controlled Self-Doping of the TiO_2(110) Surface: Combined Photoemission Spectroscopy and Density Functional Theory Study. *Phys. Rev. B* **2008**, *77*, 235424.
36. Henderson, M. A.; Epling, W. S.; Peden, C. H. F.; Perkins, C. L. Insights into Photoexcited Electron Scavenging Processes on TiO_2 Obtained from Studies of the Reaction of O_2 with OH Groups Adsorbed at Electronic Defects on TiO_2(110). *J. Phys. Chem. B* **2003**, *107*, 534–545.
37. Liu, L. M.; McAllister, B.; Ye, H. Q.; Hu, P. Identifying an O_2 Supply Pathway in CO Oxidation on Au/TiO_2(110): A Density Functional Theory Study on the Intrinsic Role of Water. *J. Am. Chem. Soc.* **2006**, *128*, 4017–4022.
38. Meyer, R.; Lemire, C.; Shaikhutdinov, S. K.; Freund, H. Surface Chemistry of Catalysis by Gold. *Gold Bull.* **2004**, *37*, 72–124.
39. Sivadinarayana, C.; Choudhary, T. V.; Daemen, L. L.; Eckert, J.; Goodman, D. W. The Nature of the Surface Species Formed on Au/TiO_2 during the Reaction of H_2 and O_2: An Inelastic Neutron Scattering Study. *J. Am. Chem. Soc.* **2004**, *126*, 38–39.
40. Qin, H.; Wenger, S.; Xu, M.; Gao, F.; Jing, X.; Wang, P.; Zakeeruddin, S. M.; Grätzel, M. An Organic Sensitizer with a Fused Dithienothiophene Unit for Efficient and Stable Dye-Sensitized Solar Cells. *J. Am. Chem. Soc.* **2008**, *130*, 9202–9203.
41. Diebold, U.; Lehman, J.; Mahmoud, T.; Kuhn, M.; Leonardelli, G.; Hebenstreit, W.; Schmid, M.; Varga, P. Intrinsic Defects on a TiO_2(110)(1 × 1) Surface and Their Reaction with Oxygen: A Scanning Tunneling Microscopy Study. *Surf. Sci.* **1998**, *411*, 137–153.
42. Onishi, H.; Iwasawa, Y. STM-Imaging of Formate Intermediates Adsorbed on a TiO_2(110) Surface. *Chem. Phys. Lett.* **1994**, *226*, 111–114.
43. Kurtz, R. L.; Stockbauer, R.; Madey, T. E.; Román, E.; de Segovia, J. L. Synchrotron Radiation Studies of H_2O Adsorption on TiO_2(110). *Surf. Sci.* **1989**, *218*, 178–200.
44. Teobaldi, G.; Hofer, W. A.; Bikondoa, O.; Pang, C. L.; Cabailh, G.; Thornton, G. Modelling STM Images of TiO_2(110) From First-Principles: Defects, Water Adsorption and Dissociation Products. *Chem. Phys. Lett.* **2007**, *437*, 73–78.
45. Du, Y.; Dohnálek, Z.; Lyubinetsky, I. Transient Mobility of Oxygen Adatoms upon O_2 Dissociation on Reduced TiO_2(110). *J. Phys. Chem. C* **2008**, *112*, 2649–2653.
46. Epling, W. S.; Peden, C. H. F.; Henderson, M. A.; Diebold, U. Evidence for Oxygen Adatoms on TiO_2(110) Resulting From O_2 Dissociation at Vacancy Sites. *Surf. Sci.* **1998**, *412/413*, 333–343.
47. Henderson, M. A.; White, J. M.; Uetsuka, H.; Onishi, H. Photochemical Charge Transfer and Trapping at the Interface between an Organic Adlayer and an Oxide Semiconductor. *J. Am. Chem. Soc.* **2003**, *125*, 14974–14975.
48. Hugenschmidt, M. B.; Gamble, L.; Campbell, C. T. The Interaction of H_2O with a TiO_2(110) Surface. *Surf. Sci.* **1994**, *302*, 329–340.
49. https://wiki.fysik.dtu.dk/dacapo.
50. Hammer, B.; Hansen, L. B.; Nørskov, J. K. Improved Adsorption Energetics within Density-Functional Theory Using Revised Perdew-Burke-Ernzerhof Functionals. *Phys. Rev. B* **1999**, *59*, 7413–7421.
51. Bennett, R. A. The Re-Oxidation of the Substoichiometric TiO_2(110) Surface in the Presence of Crystallographic Shear Planes. *PhysChemComm.* **2000**, *3*, web-based journal.
52. Rohrer, G. S.; Henrich, V. E.; Bonnell, D. A. Structure of the Reduced TiO_2(110) Surface Determined by Scanning Tunneling Microscopy. *Science* **1990**, *250*, 1239–1241.
53. Tilocca, A.; DiValentin, C.; Selloni, A. O_2 Interaction and Reactivity on a Model Hydroxylated Rutile (110) Surface. *J. Phys. Chem. B* **2005**, *109*, 20963–20967.
54. Tersoff, J.; Hamann, D. R. Theory of Scanning Tunneling Microscopy. *Phys. Rev. B* **1985**, *31*, 805–813.
55. Daté, M.; Okumura, M.; Tsubota, S.; Haruta, M. Vital Role of Moisture in the Catalytic Activity of Supported Gold Nanoparticles. *Angew. Chem., Int. Ed.* **2004**, *43*, 2129–2132.
56. Knapp, M.; Crihan, D.; Seitsonen, A. P.; Over, H. Hydrogen Transfer Reaction on the Surface of an Oxide Catalyst. *J. Am. Chem. Soc.* **2005**, *127*, 3236–3237.
57. Knapp, M.; Crihan, D.; Seitsonen, A. P.; Resta, A.; Lundgren, E.; Anderson, J. N.; Schmid, M.; Varga, P.; Over, H. Unusual Process of Water Formation on RuO_2(110) by Hydrogen Exposure at Room Temperature. *J. Phys. Chem. B* **2006**, *110*, 14007–14010.
58. Lægsgaard, E.; Besenbacher, F.; Mortensen, K.; Stensgaard, I. A Fully Automated, 'Thimble-Size' Scanning Tunnelling Microscope. *J. Microsc.* **1988**, *152*, 663–669.
59. Lauritsen, J. V.; Besenbacher, F. Model Catalyst Surfaces Investigated by Scanning Tunneling Microscopy. *Adv. Catal.* **2006**, *50*, 97–147.
60. Lægsgaard, E.; Österlund, L.; Thostrup, P.; Rasmussen, P. B.; Stensgaard, I.; Besenbacher, F. A High-Pressure Scanning Tunneling Microscope. *Rev. Sci. Instrum.* **2001**, *72*, 3537–3542.
61. Ehrlich, G. Atomic Displacement in One- and Two-Dimensional Diffusion. *J. Chem. Phys.* **1966**, *44*, 1050–1055.
62. Bahn, S. R.; Jacobsen, K. W. An Object-Oriented Scripting Interface to a Legacy Electronic Structure Code. *Comput. Sci. Eng.* **2002**, *4*, 56–66.
63. Henkelman, G.; Uberuaga, B. P.; Jónsson, H. A Climbing Image Nudged Elastic Band Method for Finding Saddle Points and Minimum Energy Paths. *J. Chem. Phys.* **2000**, *113*, 9901–9904.